JOURNAL OF Evolutionary Biology

doi: 10.1111/jeb.13196

Phylogenomics of pike cichlids (Cichlidae: *Crenicichla*): the rapid ecological speciation of an incipient species flock

E. D. BURRESS*, F. ALDA†, A. DUARTE‡, M. LOUREIRO‡§, J. W. ARMBRUSTER* & P. CHAKRABARTY†

*Department of Biological Sciences and Auburn University Museum of Natural History, Auburn University, Auburn, AL, USA
†Museum of Natural Science, Department of Biological Sciences, Louisiana State University, Baton Rouge, LA, USA
‡Sección Zoología Vertebrados, Departmento de Ecología y Evolución, Facultad de Ciencias, Universidad de la República, Montevideo, Uruguay
§Sección Ictología, Departmento de Zoología, Museo Nacional de Historia Natural, Montevideo, Uruguay

Keywords:

adaptive radiation;
ecological speciation;
phylogeny;
ultraconserved elements.

Abstract

The rapid rise of phenotypic and ecological diversity in independent lake-dwelling groups of cichlids is emblematic of the East African Great Lakes. In this study, we show that similar ecologically based diversification has occurred in pike cichlids (*Crenicichla*) throughout the Uruguay River drainage of South America. We collected genomic data from nearly 500 ultraconserved element (UCEs) loci and >260 000 base pairs across 33 species, to obtain a phylogenetic hypothesis for the major species groups and to evaluate the relationships and genetic structure among five closely related, endemic, co-occurring species (the Uruguay River species flock; URSF). Additionally, we evaluated ecological divergence of the URSF based on body and lower pharyngeal jaw (LPJ) shape and gut contents. Across the genus, we recovered novel relationships among the species groups. We found strong support for the monophyly of the URSF; however, relationships among these species remain problematic, likely because of the rapid and recent evolution of this clade. Clustered co-ancestry analysis recovered most species as well delimited genetic groups. The URSF species exhibit species-specific body and LPJ shapes associated with specialized trophic roles. Collectively, our results suggest that the URSF consists of incipient species that arose via ecological speciation associated with the exploration of novel trophic roles.

Introduction

The rapid accumulation of ecological roles and their associated adaptations is a hallmark of adaptive radiations (Simpson, 1953; Schluter, 2000). Such rapid diversification may occur in response to ecological opportunities afforded by the colonization of novel environments (e.g. islands or lakes) that provides competitive release (Yoder *et al.*, 2010), the rise of a key innovation that permits exploration of novel regions of the adaptive landscape (Wainwright *et al.*, 2012) and/or histories of hybridization that allow clades to overcome evolutionary constraints and permit the attainment of novel adaptive opportunities (Seehausen, 2004; Meier *et al.*, 2017). Regardless, the role of ecological divergence and ultimately of ecological speciation is central to the progression of adaptive radiations. The environmental gradients along which groups diversify and specialize as well as the degree to which ecological and genetic divergence correspond, are also fundamental characteristics that provide insight into the catalysts that drive adaptive radiations.

Cichlid fishes are textbook examples of adaptive radiations (Seehausen, 2015). In particular, the species flocks of East Africa have adapted to varied environmental conditions and often subsequently diversified extensively in their morphologies and ecologies (Muschick *et al.*, 2012). In addition to the large radiations of Lakes Tanganyika, Malawi and Victoria

Correspondence: Edward D. Burress, Department of Biological Sciences and Auburn University Museum of Natural History, Auburn University, AL, USA.
Tel.: +1 828 777 3342; e-mail: edwarddburress@gmail.com

(Wagner *et al.*, 2012), smaller lacustrine radiations also exhibit ecological diversification throughout small African and Middle American lakes (Schliewen *et al.*, 2001; Barluenga *et al.*, 2006; Elmer *et al.*, 2014; Martin *et al.*, 2015; Ford *et al.*, 2016).

Cichlid radiations exhibit common themes such as specialization along the benthic-to-pelagic habitat axis, soft-bodied-to-hard-shelled prey axis and rapid transitions to herbivory (reviewed in Burress, 2015). Rapid accumulation of ecological roles during cichlid adaptive radiations has conspicuously occurred frequently in lakes and more rarely rivers, which may be due to intrinsic differences in the opportunities afforded by those environments (Seehausen, 2015). For example, river assemblages are generally immigration-assembled such that co-occurring species often represent disparate lineages rather than monophyletic groups (i.e. speciation-assembled), which is common within lakes (Seehausen, 2015). The unstable and unpredictable environmental conditions provided by rivers may favour the evolution of omnivory rather than specialization (Jepsen & Winemiller, 2002), perhaps due to reduced need for the evolution of accommodative processes such as niche partitioning (Grossman *et al.*, 1982), which may act as initial sources of diversifying selection (Shafer & Wolf, 2013). Additionally, many ecomorphs observed in lakes may be implausible evolutionary results in rivers due to niches that are uncommon or temporally unstable in fluctuating environments (Seehausen, 2015).

Cichlids either colonized South America via trans-Atlantic dispersal from Africa (Friedman *et al.*, 2013; Matschiner *et al.*, 2017) or are Gondwanan in origin (Chakrabarty, 2004; Sparks & Smith, 2005; Genner *et al.*, 2007; McMahan *et al.*, 2013). Diversification in locomotor and trophic-associated functional morphology occurred quickly after the origin of the Neotropical clade (López-Fernández *et al.*, 2013; Arbour & López-Fernández, 2014; Burress, 2016; Feilich, 2016). Perhaps the most dramatic case involved the evolution of elongate tubular bodies specialized for feeding via high ram velocity in pike cichlids (*Crenicichla*; López-Fernández *et al.*, 2013). Despite highly conserved body morphology, pike cichlids have diversified extensively in terms of craniofacial and pharyngeal jaw morphology (Burress *et al.*, 2013a, 2015; Burress, 2016). Following colonization of the La Plata Basin via stream capture with southern tributaries of the Amazon (Reclus, 1893), pike cichlids have been particularly successful, where they exhibit high degrees of endemism and species diversity (de Lucena & Kullander, 1992; Piálek *et al.*, 2012).

Our goals for this study are two-fold. First, we aim to produce a robust phylogenetic framework for all the major lineages of *Crenicichla*, including all recognized species groups and the type species (*C. macrophthalma*). The monophyly of the species groups has been supported by previous analyses with largely mitochondrial loci; however, the relationships among them remain unresolved (Kullander *et al.*, 2010; Piálek *et al.*, 2012; Fig. S1). Second, we assess the diversification of the Uruguay River species flock (URSF). We infer the relationships among five closely related species that are endemic to the Uruguay River (i.e. the URSF): *Crenicichla missioneira*, *C. minuano*, *C. hadrostigma*, *C. celidochilus* and *C. tendybaguassu*, which co-occur throughout the drainage and often form mixed species aggregations (de Lucena & Kullander, 1992; de Lucena, 2007; Serra *et al.*, 2011). These species were originally diagnosed based on combinations of morphology, colour pattern and meristics (de Lucena & Kullander, 1992; de Lucena, 2007). Subsequent molecular analyses with primarily mitochondrial loci have not resolved the relationships among these species nor supported their monophyly (Kullander *et al.*, 2010; Piálek *et al.*, 2012).

To address objective 1, we sequenced ultraconserved elements (UCEs) and used a combination of concatenated and multispecies coalescent methods of phylogenetic inference to assess relationships among major species groups and among species. We then discuss these findings in relation to those of previous studies based largely on mitochondrial loci. For objective 2, we assessed the relationships and co-ancestry within the URSF using UCEs. Additionally, to assess ecological diversification within the URSF, we employed landmark-based geometric morphometrics of the body and lower pharyngeal jaw as well as analyses of gut contents. Previous studies have hypothesized that the URSF represents a rapid trophic-based adaptive radiation (de Lucena & Kullander, 1992; Kullander *et al.*, 2010; Piálek *et al.*, 2012; Burress *et al.*, 2013a). Here, we test this hypothesis with a combination of molecular and ecological data and discuss this clade in the context of other prevalent examples of cichlid adaptive radiations that frequently arose in lakes throughout Africa and Middle America.

Materials and methods

Study species

With more than 90 valid species, *Crenicichla* is the most species-rich genus of the Cichlinae (Neotropical cichlids; Piálek *et al.*, 2015). *Crenicichla* is present in all major cis-Andean drainages, ranging across coastal Venezuela, the Guianas, the Amazon and La Plata Basin (Piálek *et al.*, 2012). *Crenicichla* is traditionally divided into five species groups (i.e. clades): the *C. lacustris*, *C. lugubris*, *C. wallacii*, *C. saxatilis* and *C. reticulata* species groups (Piálek *et al.*, 2012 and references therein). The species groups are mostly characterized by morphology (e.g. colour pattern and meristics) and geographic distribution. Most species groups occur in sympatry in the Amazon and Orinoco drainages. The *C. lacustris* species group; however, is distributed in the La Plata Basin (i.e.

Paraná and Uruguay rivers) and South Atlantic coastal drainages (de Lucena & Kullander, 1992; Kullander & Lucena, 2006; Piálek *et al.*, 2012). *Crenicichla semifasciata* (*reticulata* group), *C. britskii* (*saxatilis* group) and *C. lepidota* (*saxatilis* group) are the only species known from other species groups that also have a sub-Amazonian distribution (Kullander *et al.*, 2010; Piálek *et al.*, 2012). Although the monophyly of the five traditional species groups is generally supported, their phylogenetic relationships are uncertain (Fig. S1), as is the relationship of the type species, *C. macrophthalma*, which in previous analyses was recovered as a long branch not allied with any of the traditional species groups (Piálek *et al.*, 2012). Additionally, the position and monophyly of *Teleocichla*, which appears to be nested within *Crenicichla*, is also unresolved (Kullander *et al.*, 2010; Piálek *et al.*, 2012).

Phylogeny of *Crenicichla*

Taxon sampling

The 33 taxa selected for this study (Table S1) represent all species groups established by previous studies (Kullander *et al.*, 2010; Piálek *et al.*, 2012). The nominal species for each of the traditional species groups was included if available. Exceptions include *C. lugubris* and *C. lacustris*, but in these cases other representatives were chosen based on previously reported close relationships with the nominal species (Table S1; Kullander *et al.*, 2010; Piálek *et al.*, 2012). Three additional taxa closely related to *Crenicichla* were chosen as outgroups (López-Fernández *et al.*, 2010; McMahan *et al.*, 2013): *Acarichthys heckelii*, *Apistogramma ortmani* and *Gymnogeophagus tiraparae* (Table S1). Most samples were acquired via museum loans, some tissues were collected during field expeditions to Uruguay in 2013, and additional samples were acquired from the aquarium trade (Table S1). For the URSF, which is part of the *C. lacustris* species group, we included two to six individuals from each species for the molecular analyses. Voucher specimens are accessioned in the Auburn University Museum of Natural History (AUM), the Academy of Natural Sciences of Drexel University (ANSP) and Universidade Federal do Rio Grande do Sul (UFRGS) (Table S1).

Library preparation

We used a sequence capture method to construct 49 DNA libraries enriched for ultraconserved elements (UCEs; complete species list, their species group membership and collection locations are provided in Table S1). UCEs are segments of the genome that are highly conserved (≥100 bp and ≥80% identity) between orthologous regions of evolutionarily divergent taxa (Bejerano *et al.*, 2004; Faircloth *et al.*, 2012). These properties, together with their abundance throughout the genome, little overlap with known paralogous genes, and increasing variability in sequence flanking regions, make UCEs desirable molecular markers that have been proven useful for reconstructing deep phylogenetic relationships, as well as for comparative phylogeography and population genetics at shallower timescales (Faircloth *et al.*, 2012; Smith *et al.*, 2014; Newman & Austin, 2016).

Genomic DNA was extracted from fin or muscle tissue preserved in ethanol or RNA-later using the Omegabiotek E.Z.N.A. animal tissue extraction kit (product #D3396-02) and verified for quality and quantity using agarose gel electrophoresis and a Qubit fluorometer (Life Technologies, Waltham, MA, USA), respectively. We randomly sheared 400–1000 ng DNA by sonication to a target size of 400–600 bp using a EpiSonic Multi-Functional Bioprocessor (Epigentek, Farmingdale, NY, USA), and used it to construct DNA libraries using the Kapa Hyper Prep Kit v.3.15 (Kapa Biosystems, Wilmington, MA, USA). Instead of the standard Illumina adapters, we used adapters (12 μM) containing a custom index sequence (Faircloth & Glenn, 2012), and we used a generic SPRI substitute (Rohland & Reich, 2012; hereafter SPRI) for all cleanup steps involving magnetic beads. Following adapter ligation, we performed two cleanup steps of the ligation reaction using 0.8X SPRI, resuspended in 33 μL ddH_2O and quantified 2 μL of the resulting library using a Qubit fluorometer. We amplified 15 μL of the adapter-ligated library using a reaction mix of 25 μL 2X Kapa HiFi HotStart ReadyMix (Kapa Biosystems), 5 μL of Illumina TruSeq (San Diego, CA, USA) primer mix (5 μM each) and 5 μL of ddH_2O and the following thermal profile: 98 °C for 45 s, 10 cycles at 98 °C for 15 s, 60 °C for 30 s, 72 °C for 60 s; and a final extension of 72 °C for 5 m. We purified completed PCR using 1X SPRI and resuspended libraries in 23 μL ddH_2O, and we quantified 2 μL of each library using a Qubit fluorometer. We combined groups of eight libraries at equimolar concentrations, having a final concentration of each enrichment pool of 147 ng μL^{-1} in 7 μL (500 ng in total).

Target enrichment and sequence of UCEs

We enriched libraries using a set of 2001 probes (Actinopts-UCE-0.5Kv1) targeting 500 UCE loci across Actinopterygii (Faircloth *et al.*, 2013). We followed library enrichment procedures for the MYcroarray MYBaits kit v.3.0 (Ann Arbor, MI, USA), except that we added 500 ng custom blocking oligos designed against our custom sequence tags, and using 10 inosines to block the 10-nucleotide index sequence. We ran the hybridization reaction for 24 h at 65 °C. Following hybridization, we bound all pools to streptavidin beads (MyOne C1, Life Technologies) and washed bound libraries to remove nonhybridized and nonspecifically hybridized molecules. We added 30 μL of ddH_2O to each sample and combined 15 μL of streptavidin bead-bound enriched libraries in ddH_2O with 25 μL HiFi HotStart Taq (Kapa Biosystems), 5 μL of Illumina

TruSeq primer mix (5 μM each) and 5 μL of ddH_2O. We recovered each library by PCR using the following thermal profile: 98 °C for 2 m; 16 cycles of 98 °C for 20 s, 60 °C for 30 s, 72 °C for 60 s; and a final extension of 72 °C for 5 m. We placed the resulting PCR in a magnet stand and removed the supernatant to separate the PCR-recovered, enriched DNA (supernatant) from the streptavidin beads. We subsequently purified the enriched DNA for each pool using 1X SPRI, and we rehydrated enriched DNA in 33 μL of ddH_2O. We quantified 2 μL of each enriched pool using a Qubit fluorometer, and we diluted enriched pools to 2.5 ng μL^{-1} in 10 mM Tris–HCl. We combined five diluted enriched pools of eight samples and one pool of nine samples from this study with 12 diluted enriched pools from a separate study (146 samples in total) to create an equimolar pool-of-pooled libraries at 10 nM concentration. We sequenced 10 pmol of this mixture in one lane of PE100 sequencing on an Illumina HiSeq (University of Missouri-Columbia DNA Core Facility). Raw read data are archived in the NCBI Sequence Repository Archive (SRA; BioProject ID PRJNA396208), and concatenated and individual gene alignments are archived on Dryad (doi:10.5061/dryad.7qs13).

Analysis of captured sequence data

We preprocessed demultiplexed sequences and prepared them for analyses using programs in the PHYLUCE package (Faircloth, 2016) available at http://github.com/faircloth-lab/phyluce. We trimmed reads to remove adapter contamination and low-quality bases using a parallel wrapper (https://github.com/faircloth-lab/illumiprocessor) around *trimmomatic* (Bolger *et al.*, 2014), and assembled cleaned reads using a parallel wrapper around *trinity* (trinityrnaseq-r2013-02-25; *phyluce_assembly_assemblo_trinity.py*; Grabherr *et al.*, 2011; Marcais & Kingsford, 2011).

To identify assembled contigs representing enriched UCE loci, we aligned species-specific contig assemblies to a FASTA file of all enrichment baits using *phyluce_assembly_match_contigs_to_probes.py*. This program implements the matching process using LASTZ and ensures that matches are 80% identical over 80% of their length. This program also screens and removes potential duplicate contigs or contigs that are hit by baits targeting more than one UCE locus. After screening and removing nontarget and duplicated or misassembled contigs, the program creates a relational database containing several tables that map the contig names generated by the assembler to the names of each corresponding UCE locus across all taxa. We used the program *phyluce_assembly_get_match_counts.py* to query the relational database and generate two lists: one containing those loci having data for all taxa (a complete data matrix) and another containing all loci having data for any taxon (an incomplete data matrix). We input these lists of loci to an additional program (*phyluce_assembly_get_fastas_from_match_counts.py*) to create separate monolithic FASTA files matching the locus lists for complete and incomplete UCE data matrices. We exploded each monolithic FASTA by locus, and we aligned sequence data for loci containing more than four taxa using *phyluce_align_seqcap_align.py* and MAFFT (Katoh & Standley, 2013). Following alignment, we removed the locus names from all alignments using *phyluce_align_remove_locus_name_from_nexus_lines.py*.

For the complete UCE data matrix, we computed alignment statistics and the number of informative sites across all alignments using *phyluce_align_get_align_summary_data.py* and *phyluce_align_get_informative_sites.py*; we concatenated the resulting alignments into a PHYLIP-formatted supermatrix (*phyluce_align_format_nexus_files_for_raxml.py*). For the incomplete matrix, we filtered the entire set of aligned loci to create three different incomplete matrices: a 95% complete matrix (alignments contained ≥46 of 49 individuals), an 80% complete matrix (alignments contained ≥39 of 49 individuals) and a 50% complete matrix (alignments contained ≥24 of 49 individuals). Following alignment filtering, we computed alignment statistics and the number of informative sites across all alignments, and we concatenated the resulting alignments into a PHYLIP supermatrix.

Analysis of concatenated UCE data

For all data matrices, we estimated the best-fitting locus-specific site rate substitution models using Cloudforest (Crawford & Faircloth, 2014) and partitioned the UCEs by their best-fitting substitution models. We conducted 20 maximum-likelihood (ML) searches for the phylogenetic tree that best fit the data using the best-fitting partitioning scheme using RAxML v. 8.0.19 (Stamatakis, 2006) and the GTRGAMMA model. Nodal support was assessed by 500 nonparametric bootstrap replicates. We used Bayesian analyses for phylogenetic inference as implemented in MrBayes 3.1 (Huelsenbeck & Ronquist, 2001; Ronquist & Huelsenbeck, 2003), and ran four independent Markov chains of 5×10^6 generations. We sampled trees every 500 iterations to yield 10 000 trees and discarded 25% as burnin. Convergence was confirmed by checking effective sampling size values >200 in TRACER (Rambaut *et al.*, 2014), and by ensuring the average standard deviation of split frequencies was <1%, and the potential scale reduction factor (PSRF) for estimated parameters was 1.0.

In addition to the analysis and representation of evolutionary relationships using phylogenetic trees, network methods provide a useful tool for phylogenetic analysis and visualization of reticulate relationships among taxa and possible mixed ancestry or hybrid individuals. We constructed a neighbour-net analysis using ML distances inferred from concatenated UCE sequence data in Splitstree v.4.12.3 (Huson & Bryant, 2006), and performed 1000 bootstrap replicates to assess support. We also tested for recombination using the Φ statistic.

Species tree analysis

We inferred a species tree of *Crenicichla* using SVDquartets (Chifman & Kubatko, 2014, 2015) as implemented in PAUP version 4.0a150 (Swofford, 2003). The SVDquartet method does not rely on prior inference of individual gene trees; rather, it uses single-site patterns to estimate the species tree in a way that is statistically consistent with the multispecies coalescent. The algorithm takes multilocus SNP data to infer quartet trees for subsets of four species in a coalescent framework, and then combines the set of quartet trees into a species tree using a supertree method (Chifman & Kubatko, 2014). We evaluated 100 000 random quartets and performed 1000 bootstrap replicates of the data to assess support, and then assembled the species tree using the quartet max-cut method (Snir & Rao, 2012).

Genetic structure and ecological diversification of the Uruguay River species flock

Genetic structure analysis

We investigated the genetic structure among species within the URSF using the Markov chain Monte Carlo (MCMC) clustering algorithm implemented in the program fineRADstructure (Malinsky *et al.*, 2016). This program is a modified version of the fineSTRUCTURE package (Lawson *et al.*, 2012), which uses haplotype linkage information of the sequence of all single nucleotide polymorphisms (SNPs) to calculate a co-ancestry matrix based on the most recent coalescence (i.e. the closest relatives for each allele) among sampled individuals, but as opposed to fineSTRUCTURE it does not require information on the chromosomal location of the markers or phased haplotypes. In our case, we assumed perfect linkage among SNPs within each UCE locus and frequent recombination between loci.

To identify SNPs and indels from our UCE data, we created a reference dictionary for one of our samples using Picard (http://broadinstitute.github.io/picard/), and indexed the reference using SAMtools (Li *et al.*, 2009). We then aligned all our read data to the reference using bwa (Li & Durbin, 2009), and the output SAM files were converted into BAM format using SAMtools. We removed duplicate reads using Picard, to ensure that all our fragments have been independently targeted. We merged all the individual BAM files and realigned them around the indels using IndelRealigner in the Genome Analysis Toolkit (GATK; McKenna *et al.*, 2010). We then called SNPs and indels using VariantAnnotator. We masked indels and removed SNPs with a quality score below Q30 using VariantFiltration. We outputted the 1148 passing SNPs into a vcf file and transformed it into a Tag Haplotype Matrix using the Python program vcf2hapmatrix.py (available at https://github.com/pimbongaerts/radseq). We used the Tag Haplotype Matrix as input for the program RADpainter, included in the fineRADstructure package, to calculate the co-ancestry matrix. We assigned individuals to populations using fineSTRUCTURE by running the MCMC for 100 000 generations following an initial 100 000 generations that were discarded as burnin. We visualized and plotted the results using R scripts fineRADstructurePlot.R and FinestructureLibrary.R (available at http://cichlid.gurdon.cam.ac.uk/fineRADstructure.html).

Body and pharyngeal jaw shape analysis

We quantified body and lower pharyngeal jaw (LPJ) shape of the five species within the URSF using museum collections at the Auburn University Museum of Natural History and Universidad Federal do Rio Grande do Sul (Table S2): *Crenicichla celidochilus* ($N = 12$), *C. hadrostigma* ($N = 6$), *C. minuano* ($N = 19$), *C. missioneira* ($N = 24$) and *C. tendybaguassu* ($N = 7$). Only specimens that represented adult size classes were included to avoid confounding effects of ontogeny (i.e. Burress *et al.*, 2013b). We photographed specimens in lateral view using a mounted Nikon D5100 digital camera (Nikon Corporation, Tokyo, Japan). Additionally, we dissected, cleaned and photographed the LPJ in dorsal aspect. To quantify body shape, we used 15 homologous and 10 sliding landmarks that describe ecologically meaningful shape variation (Fig. S2a). The placements of sliding landmarks emphasize the craniofacial region because of the hypothesized importance of trophic-based diversification within the URSF (i.e. Piálek *et al.*, 2012; Burress *et al.*, 2013a). We used four homologous and 18 sliding landmarks that describe the shape of the LPJ (Fig. S2b). Sliding landmarks are not associated with a homologous structure, but quantify the curvature between two homologous landmarks. All analyses were performed with the tps program suite. Photographs were consolidated and landmarked using tpsUtil (Rohlf, 2004) and tpsDIG2 (Rohlf, 2006), respectively. Landmarks were superimposed and aligned and relative warps were generated using tpsrelw (Rohlf, 2007). Relative warps are principal components of shape variation and describe the major axes of shape variation among individuals. Scale, rotation and translation were removed from the analysis during superimposition and generation of the Procrustes fit.

To estimate the direction and magnitude of body and LPJ shape change along branches of the URSF phylogeny, we reconstructed a population-level phylomorphospace (Sidlauskas, 2008) by overlaying the ML phylogeny onto the PC biplots of body and LPJ shape. For this procedure, we pruned the set of PC scores to include only the UCE voucher specimens (Table S1). We mapped the phylogeny onto body, and LPJ PC scores using Mesquite v2.75 (Maddison & Maddison, 2011). The values of internal nodes were calculated using weighted squared-change parsimony (Maddison, 1991; Revell *et al.*, 2007).

Gut content analysis

We summarized the diets of four URSF species: *C. celidochilus* ($N = 30$), *C. tendybaguassu* ($N = 26$), *C. minuano* ($N = 37$) and *C. missioneira* ($N = 44$) based on previous studies (Burress, 2012; Burress *et al.*, 2013a, 2015). Using the same methods, we also analysed the diet of *C. hadrostigma* ($N = 15$). We quantified the relative proportions of prey items as described by Winemiller (1989). We removed, sorted, identified and measured the contents from the anterior half of the digestive tract in appropriately sized graduated cylinders. For small items (e.g. insect fragments), we spread sorted material onto slides and compared its area to a substance of a known volume. Prey items were pooled into five generalized categories: fishes, insects, molluscs, crustaceans and periphyton. The periphyton category includes filamentous algae, diatoms and amorphic vegetation.

We calculated niche overlap based on the relative volumetric proportions of these five prey items using Schoener's (Schoener, 1970) and Pianka's (Pianka, 1973) indices. Both indices represent the degree of niche overlap between species pairs, where 0 represents total separation and 1 represents total overlap. Generally, high overlap is depicted by overlap values >0.6, whereas low overlap is depicted by values <0.4; however, some indices tend to underestimate or overestimate overlap (Grossman, 1986). The Schoener's and Pianka's indices should depict the range between low and high estimates of niche overlap, respectively (Grossman, 1986). Pairwise niche overlap calculations were performed using the 'spaa' R package (Gotelli, 2000; Zhang, 2004).

Results

Phylogenomic analysis of UCEs

We sequenced >53 million reads with a mean of 1 159 614 reads per sample from 46 individuals representing 33 species of *Crenicichla* (Table 1). We assembled a mean of 3585.8 contigs per sample (Table 1). The resulting data matrices included (1) a 100% complete matrix containing 31 loci having a mean length of 611.0 bp per loci, totalling 18 964 bp of aligned sequence; (2) a 95% complete matrix containing 248 loci having a mean length of 607.47 bp per loci, totalling 150 654 bp of aligned sequence; (3) a 80% complete matrix containing 427 loci having a mean length of 573.97 bp per loci, totalling 245 084 bp of aligned sequence; and (4) a 50% complete matrix containing 465 loci having a mean length of 561.6 bp, totalling 261 143 bp of aligned sequence (Table 2).

The phylogeny of *Crenicichla*

The inferred phylogenomic hypothesis of *Crenicichla* (Fig. 1) was consistent between concatenated phylogenetic methods and across data sets with different levels of missing data (Figs S3 and S4). The monophyly of all the species groups was highly supported across all analyses and data sets (bootstrap support, BS ≥ 99; Bayesian posterior probabilities, PP = 1.0), except for the 100% complete data set, which did not recover the *C. lugubris* species group with high support (BS = 53, PP = 0.82). Similarly, relationships among species groups were only resolved with high support in data sets that included over 400 loci (i.e. 80% and 50% completeness). We recovered two main lineages of *Crenicichla*, the first of which included the *C. lacustris* and *C. reticulata* species groups (Figs S3 and S4), and the type species, *C. macrophthalma*, which was always recovered as the sister taxon to the *C. reticulata* group (BS ≥ 80, PP = 1.0) (Figs S3 and S4), except in the 100% complete matrix, where *C. macrophthalma* was recovered as the sister group to the *C. lacustris* species group, but only with moderate support (BS=78, PP=0.77). The second lineage was formed by the *C. saxatilis* and *C. lugubris* species groups, which always constituted sister clades, and the *C. wallacii* group, which was the sister group to them (Figs S3 and S4), except in the ML and BI 100% complete data set and the ML 95% complete data set (Figs S3 and S4). *Teleocichla* was recovered as the sister group to the clade formed by the *C. saxatilis*, *C. lugubris* and *C. wallacii* species groups (Figs S3 and S4), except in the ML 100% and 95% complete data sets in which *Teleocichla* was recovered as the sister group to the *C. wallacii* species group with poor support, and the BI 100% complete data set that recovered *Teleocichla* as the sister group to *C. wallacii* with high support (PP = 0.94).

The species trees inferred using SVDquartets were highly consistent with the concatenated phylogenetic methods (Fig. 1) and across data sets, except for the 100% complete data set, which did not recover the *C. lugubris* and *C. saxatilis* species groups as reciprocally monophyletic, or any of the relationships within species groups with high support (Fig. S5). Also, *Teleocichla* was recovered as the sister group to all *Crenicichla sensu stricto* using the 100% complete matrix, but was recovered as the sister group to the clade containing the *C. wallacii*, *C. saxatilis* and *C. lugubris* species groups in the 95%, 80% and 50% matrices (Fig. S5). All the remaining relationships between species groups, as well as species-level relationships within groups, were identical between ML, BI and species tree analyses, and across 95%, 80% and 50% complete data matrices (Figs S3, S4 and S5).

The evolution and ecological diversification of the Uruguay River species flock

Phylogeny and genetic structure

The URSF was monophyletic in all the concatenated ML and BI analyses (BS = 100, PP = 1.0). The relationships among species within the URSF were mostly unresolved and differed between methods and data

Table 1 Summary information, including number of reads and contigs, contig lengths and number of loci recovered for all the samples analysed.

Species	ID	Reads	Contigs	Mean contig length	SD	Min. contig length	Max. contig length	Loci
Crenicichla acutirostris	CRAC	1 359 076	3602	1859.5	5881.6	224	74 128	438
Crenicichla albopunctata	CRALB4786	943 452	3221	540.9	601.7	224	16 615	426
Crenicichla alta	CRALT1408	1 812 649	6217	445.8	460.8	224	16 576	450
Crenicichla cf. reticulata	CRBC	1 246 632	3457	529.8	576.7	224	10 796	431
Crenicichla celidochilus	CRCE2237	2 583 739	8372	452.4	449.9	224	15 450	434
Crenicichla celidochilus	CRCE2238	675 831	2297	459.8	334.8	224	4975	452
Crenicichla celidochilus	CRCE2239	682 324	2323	479.1	410.9	224	5018	455
Crenicichla cincta	CRCI	2 514 513	8276	459.3	465.3	224	16 096	424
Crenicichla compressiceps	CRCO	1 179 436	3099	508.2	423.8	224	6168	394
Crenicichla hadrostigma	CRHA1597A	1 195 057	3481	530.7	505.1	224	13 162	423
Crenicichla hadrostigma	CRHA1597B	702 898	2172	501.5	479.2	224	15 477	433
Crenicichla hadrostigma	CRHA1597C	1 832 045	5303	485.2	487.4	224	16 216	422
Crenicichla hadrostigma	CRHA1597D	866 306	2650	529.1	512.4	224	16 424	435
Crenicichla iguapina	CRIG4703	1 329 632	3447	483.5	460.2	224	16 468	430
Crenicichla jegui	CRJE	736 894	2396	502.4	551.7	224	9346	448
Crenicichla lepidota	CRLE2244	1 335 951	3918	510.2	473.8	224	8206	420
Crenicichla lenticulata	CRLEN	2 092 557	6368	502.8	533.7	224	8820	438
Crenicichla macrophthalma	CRMAC196998	633 846	2184	496.8	465.8	224	14 096	441
Crenicichla maculata	CRMACU3462	947 048	2458	494.9	560.8	224	16 662	439
Crenicichla marmorata	CRMAR40588	894 303	2748	471.1	488.5	224	14 122	453
Crenicichla minuano	CRMN2209	272 073	1078	465.2	302.9	224	3751	428
Crenicichla minuano	CRMN2240	1 322 722	3979	507.4	438.7	224	4837	418
Crenicichla missioneira	CRMS2201	986 827	3126	484.7	413.9	224	5743	428
Crenicichla missioneira	CRMS2211	765 869	2258	534.8	483.9	224	4880	437
Crenicichla missioneira	CRMS2221	845 254	2458	523.9	414.3	224	5476	430
Crenicichla missioneira	CRMS2226	371 889	1485	439	394	224	4493	438
Crenicichla missioneira	CRMS2249	1 047 233	2989	496.7	455.8	224	5503	444
Crenicichla missioneira	CRMS2256	453 737	1476	488.1	421.3	224	4504	436
Crenicichla multispinosa	CRMU189593	585 006	1633	542.8	503.8	224	5424	449
Crenicichla percna	CRPE193085	480 653	1672	492	360	224	4130	427
Crenicichla punctata	CRPU2266	2 006 012	6326	471	478.1	224	12 936	426
Crenicichla regani	CRREG	2 772 521	10280	470.1	503.8	224	15 765	411
Crenicichla saxatilis	CRSA2274	1 373 904	3967	556.2	610	224	14 068	422
Crenicichla scottii	CRSC2242	1 876 474	5892	458.1	434.5	224	13 075	425
Crenicichla sveni	CRSV	755 514	2561	479.2	363.2	224	4311	447
Crenicichla tendybaguassu	CRTE	1 619 091	4958	499.1	492.6	224	15 660	416
Crenicichla tendybaguassu	CRTE2	1 588 618	4759	508.1	586.7	224	16 700	438
Crenicichla tendybaguassu	CRTE3	1 285 162	4137	484	453.4	224	15 498	425
Crenicichla vittata	CRVI2225	1 986 172	6378	452.4	427.6	224	16 416	420
Crenicichla wallacii	CRWA3446	1 489 718	4481	563.3	595.7	224	15 970	347
Crenicichla sp. Xingu II	CRX2196400	189 640	873	468.9	433	224	3479	295
Crenicichla sp. Xingu III	CRX3193066	693 241	2134	513.7	587.2	224	14 190	447
Crenicichla zebrina	CRZE	755 317	2226	525.1	473.2	224	6029	451
Teleocichla sp. CI	TECI194669	349 138	1187	4304	289	224	4329	424
Teleocichla gephyrogramma	TEGE40123	1 021 798	2502	481.6	433	224	8511	434
Teleocichla preta	TEPR194913	884 494	2141	502.3	435.5	224	11 715	426
Acarichthys heckelii	ACHE3348	652 067	2772	522.1	628	224	16 571	448
Apistgroamma ortmanni	APOR2145	689 165	2687	471.9	339.2	224	5929	448
Gymnogeophagus tiraparae	GYTI2204	256 301	877	412.3	266	224	4302	404

matrices (Fig. 2). In general, higher levels of support and monophyly were recovered with increasing number of loci (i.e. decreasing levels of matrix completeness) and were also higher for the BI than for the ML analyses (Fig. 2a,b). For example, using the 100% complete data matrix, only *C. celidochilus* and *C. tendybaguassu* were recovered as monophyletic in the BI analysis (Fig. 2b). With the 80% and 50% complete data set, *C. hadrostigma* was also recovered as monophyletic, with strong support, in the ML and BI analyses (Fig. 2a,b). Using the 80% complete data, *C. missioneira* was also recovered as monophyletic in the

Table 2 Summary information including number of individuals and loci, locus length, polymorphic and parsimony informative sites for each of the data set.

Data set completeness	Individuals	Loci	Locus length				Polymorphic sites				Parsimony informative sites			
			Mean	SD	Range	Total	Mean	SD	Range	Total	Mean	SD	Range	Total
100%	49	31	611	74.47	486–761	18 964	24.97	18.35	8–84	774	9.13	7.31	0–31	283
95%	46	248	607.47	84.06	324–777	150 654	31.85	23.11	2–129	7898	12.18	9.45	0–56	3022
80%	39	427	573.97	104.77	254–777	245 084	33.19	22.76	2–131	14 163	12.81	9.472	0–56	5472
50%	24	465	561.6	113.35	254-777	261 143	557.62	113.27	2–131	259 294	12.6	9.42	0–56	5861

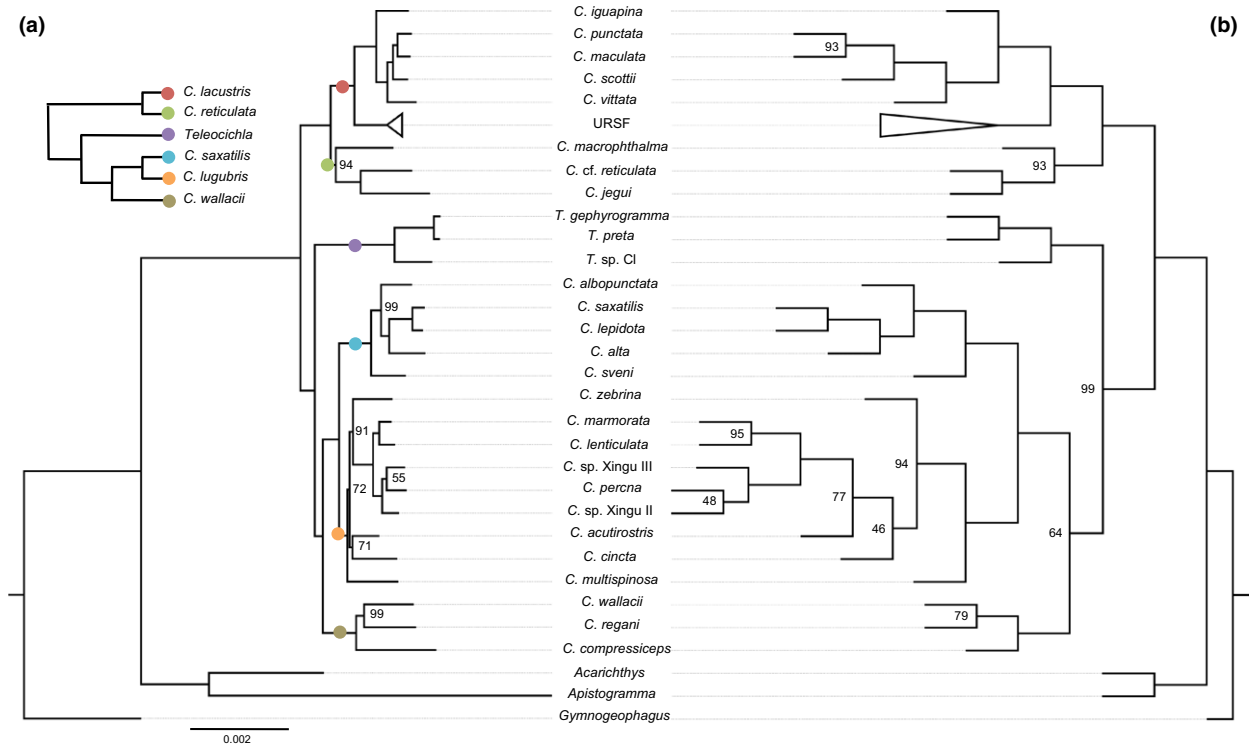

Fig. 1 *Crenicichla* phylogenomic hypotheses based on maximum-likelihood analysis of the concatenated data set (a) and SVDquartets species tree analysis (b). All nodes have 100 bootstrap supports unless otherwise noted. Analyses are based on the 80% complete data matrix (see Table 2). For relationships within the Uruguay River species flock (URSF), see Fig. 2. Inset summarizes relationships among species groups. The scale bar is in units of substitutions per site.

BI analysis (PP = 0.95; Fig. 2b). Relationships among species were also unresolved in the species trees across all data matrices (Fig. 2c).

The network constructed from the concatenated UCE data resulted in highly supported monophyletic groups (BS ≥ 92) for *C. tendybaguassu*, *C. celidochilus* and *C. hadrostigma*. On the other hand, the network showed a lack of differentiation with respect to *C. missioneira* and *C. minuano* and evidenced the reticulated nature of the relationships between these two species (Fig. 2d). No statistical support for recombination was recovered (all loci $P \geq 0.26$).

These results are consistent with the clustered co-ancestry analysis in fineRADstructure, where the most distinct clusters and largest amounts of co-ancestry were obtained for *C. tendybaguassu* and *C. celidochilus* (Fig. 3). Overall, all the species of the URSF were assigned to distinct genetic clusters that share larger co-ancestry levels within clusters, than between them. Between species, the largest amount of shared co-ancestry was found between *C. missioneira* and *C. minuano*, whereas the lowest level of co-ancestry sharing was found between *C. hadrostigma* and *C. celidochilus*. Additionally, and despite the low sampling size, there

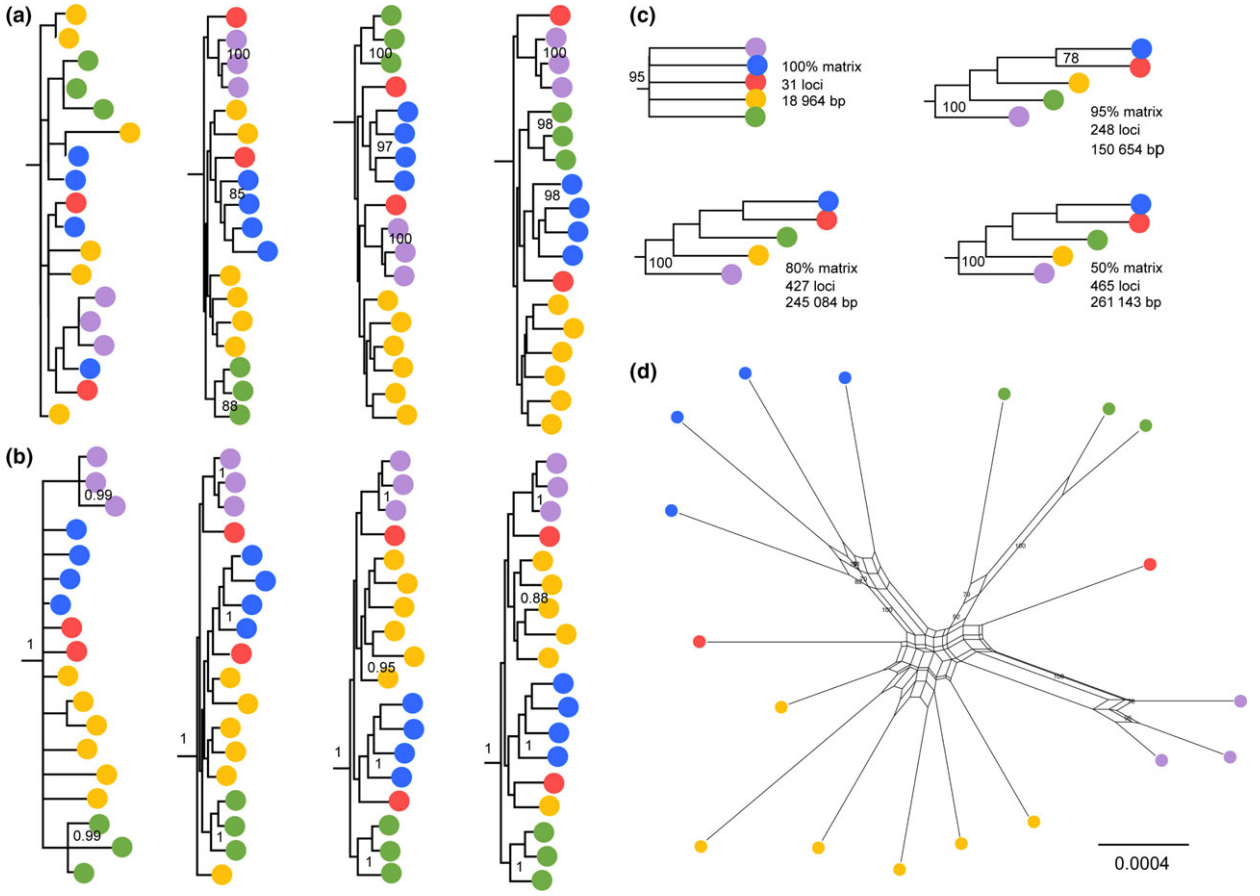

Fig. 2 Phylogenetic relationships based on concatenated maximum likelihood (a), Bayesian inference (b) and SVDquartets species trees (c) within the Uruguay River species flock (URSF) across matrices with varying proportions of missing data (see Table 2): *Crenicichla celidochilus* (purple), *C. hadrostigma* (blue), *C. minuano* (red), *C. missioneira* (yellow) and *C. tendybaguassu* (green). Only bootstrap values >70 and PP > 0.85 supporting the monophyly of species in the URSF are shown. Splitstree network representation of the relationships among species in the URSF (d).

appears to exist some degree of population substructure in *C. tendybaguassu* and *C. hadrostigma* (Fig. 3).

Body and lower pharyngeal jaw shape

Analysis of body shape resulted in the first two PCs collectively explaining 49.5% of the body shape variation among individuals. Principal component 1 explained 29.3% of the body shape variation and described variation in the relative length and depth of the head, body depth and orientation of the snout and mouth (Fig. 4a). Principal component 2 explained 20.2% of the body shape variation and mainly described variation in relative body depth (Fig. 4a). Species were primarily discriminated along PC1 (Fig. 4a). On one extreme, *C. celidochilus* and *C. missioneira* had elongated heads and terminal mouths, whereas on the other extreme, *C. hadrostigma* had a short head and benthic-oriented snout and mouth. *Crenicichla minuano* also had a short head, but a terminal mouth, and *C. tendybaguassu* had an intermediate head length and shallow body (Fig. 4a). Analysis of LPJ shape resulted in the first two PCs collectively explaining 95.2% of the LPJ shape variation among individuals. Principal component 1 explained 83.5% of the shape variation and described variation in the relative length of the medial and lateral processes (Fig. 4b). Principal component 2 explained 11.7% of the shape variation and described variation in the orientation of the lateral processes (Fig. 4b). Species exhibited species-specific LPJ shapes that were particularly discrete along PC1. *Crenicichla celidochilus* as well as *C. missioneira* had relatively atrophied LPJs with long and widely spaced lateral processes. In contrast, *C. minuano* had hypertrophied LPJs with short robust medial and lateral processes (Fig. 4b). *Crenicichla hadrostigma* had a somewhat robust LPJ with short widely spaced lateral processes and a short medial process, whereas *C. tendybaguassu* had intermediately long lateral processes and a long medial process (Fig. 4b).

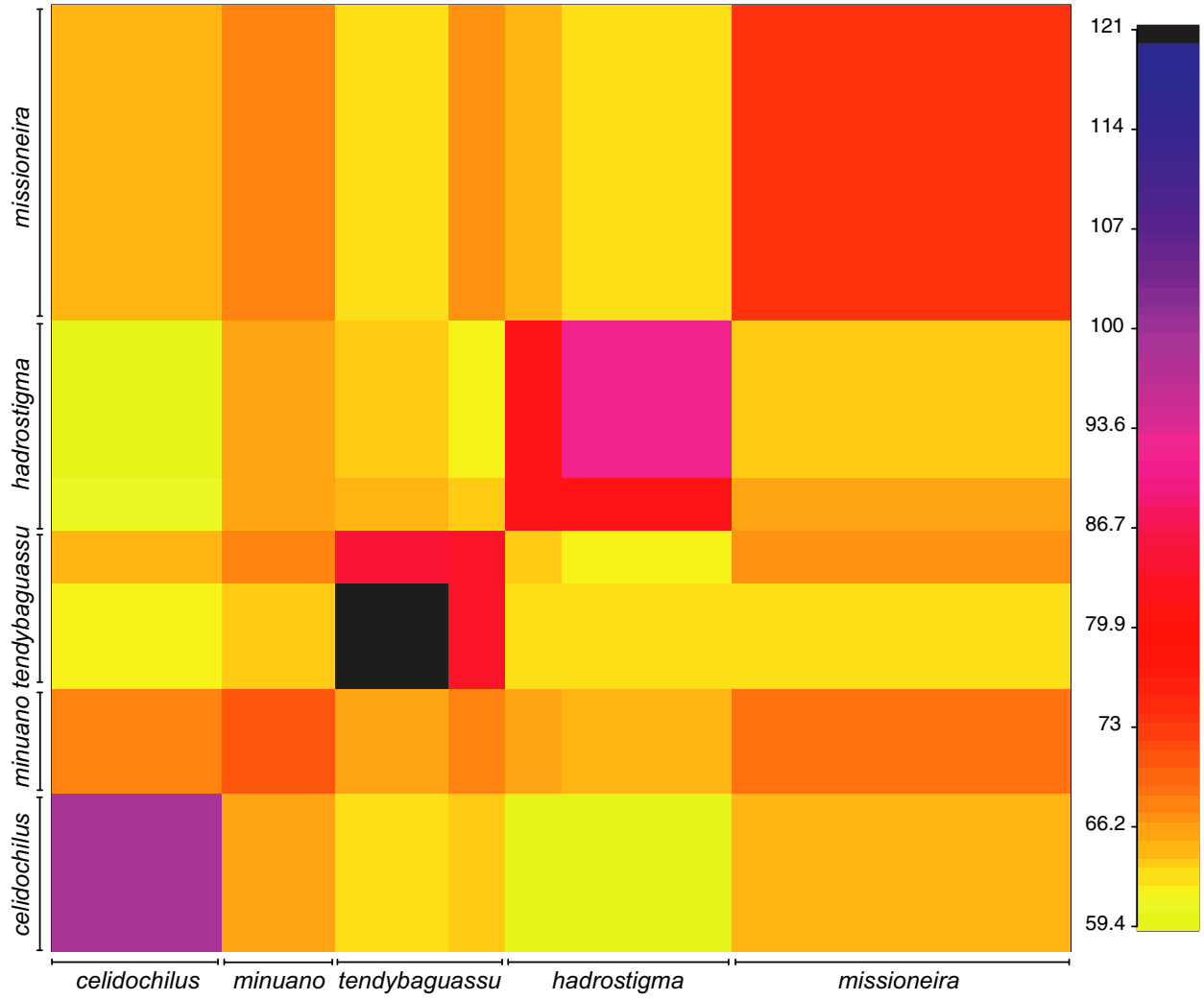

Fig. 3 Clustered fineRADstructure co-ancestry matrix. The highest levels of co-ancestry are indicated in black and purple. The lowest levels of co-ancestry sharing are indicated by yellow colours.

Population-level phylomorphospace indicates that some species, such as *Crenicichla hadrostigma* and *C. tendybaguassu*, exhibit little body and LPJ shape variation among populations (Fig. 4c,d). *Crenicichla celidochilus* exhibits more variation in LPJ shape among populations than in body shape (Fig. 4c,d). The *C. minuano* population from the Cuareim River Basin were deeper-bodied than those from the Negro River Basin (Fig. 3c). The *C. missioneira* populations from the Uruguay and Queguay rivers were more elongated than those from the other populations (Fig. 4c), whereas populations from the Cuareim, Uruguay, Queguay and Negro rivers had LPJs with more widely spaced lateral processes (Fig. 4d).

Gut contents

Gut contents were different among species, particularly in the relative consumption of fishes, molluscs and periphyton (Fig. 4e). *Crenicichla missioneira* consumed primarily fishes, but also insects and crustaceans (Fig. 4e). The remaining four species specialized on specific types of prey. *Crenicichla celidochilus* consumed almost exclusively fishes (i.e. 91% by volume). In contrast, *C. minuano* consumed primarily molluscs (i.e. bivalves and snails; 73% by volume; Fig. 4e). *Crenicichla tendybaguassu* consumed almost exclusively insects (i.e. 90% by volume; Fig. 4e), and *C. hadrostigma* also consumed primarily insects, but was the only species to consume a large fraction of periphyton (i.e. 26% by volume; Fig. 4e). Schoener's and Pianka's measures of niche overlap indicated that most pairwise dietary overlaps were low, with the exception of high overlap between *C. missioneira* and *C. celidochilus* and between *C. hadrostigma* and *C. tendybaguassu* (Table 3).

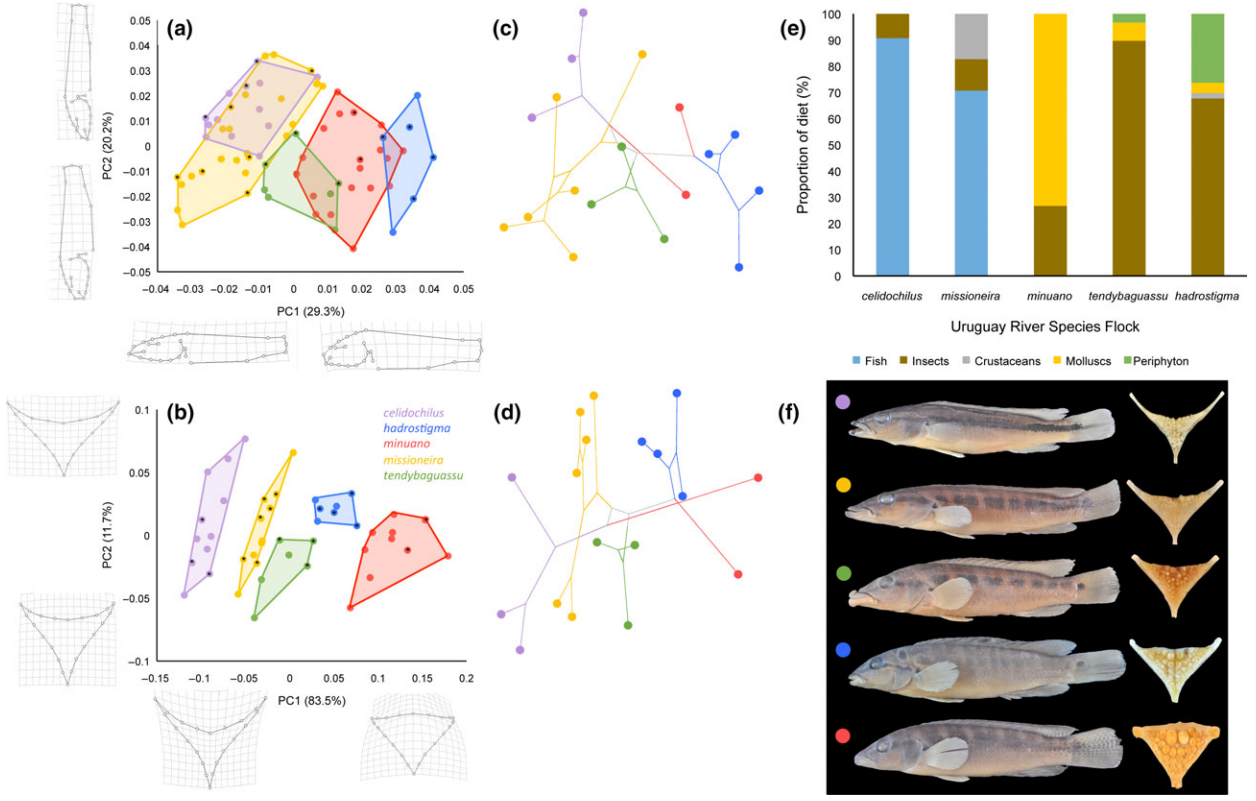

Fig. 4 Body (a) and lower pharyngeal jaw (LPJ; (b) shape among members of the Uruguay River species flock. Wire frames depict the shape changes along each axis. Asterisks depict individuals used in phylogenomic analyses. Population-level phylomorphospace depicting the direction and magnitude of body (c) and LPJ (d) shape change along branches of the maximum-likelihood phylogeny. Each point represents an individual. Phylomorphospace is based on a reduced data set including only the voucher specimens used in the UCE analyses (those denoted with asterisks in panels a,b). Bar plot summarizing gut content analyses of the URSF (e). Representatives of the body and LPJ morphologies of the URSF (f): *Crenicichla celidochilus* (purple), *C. missioneira* (yellow), *C. tendybaguassu* (green), *C. hadrostigma* (blue) and *C. minuano* (red).

Discussion

Phylogenomics of *Crenicichla*

We inferred a phylogenomic hypothesis that is in part consistent with previous morphological and molecular studies. Our phylogeny recovers all *Crenicichla* species groups as monophyletic, but includes novel relationships among species groups. These relationships were well supported and consistent across phylogenetic methods and varying levels of missing data.

The five species groups within *Crenicichla* were recognized based on morphology, colour pattern and meristics (Piálek *et al.*, 2012 and references therein). Previous molecular studies support the monophyly of these species groups; however, they exhibit disagreement about the relationships among them (Fig. S1). We recovered novel relationships among the major species groups; it is most noteworthy that the type species, *C. macrophthalma*, has a sister relationship with the *C. reticulata* species group. This result was consistent between concatenated (ML and BI) and species tree analyses, and across matrices of various degrees of missing data (Figs S3, S4 and S5). In previous studies, the position of *C. macrophthalma* was either completely unresolved (i.e. Kullander *et al.*, 2010) or recovered as the sister lineage to the *C. lacustris* species group (i.e. Piálek *et al.*, 2012). *Crenicichla macrophthalma* is an Amazonian species; thus, geographically, being allied with a species group consisting of almost exclusively Amazonian species (i.e. the *C. reticulata* species group) is more likely than being allied with species group consisting of exclusively subtropical species (i.e. the *C. lacustris* species group).

The positions of the *C. wallacii* species group and *Teleocichla* clade have been particularly problematic in previous studies based largely on mitochondrial loci (Kullander *et al.*, 2010; Piálek *et al.*, 2012). *Teleocichla* was originally distinguished from *Crenicichla* based on morphology, such as their curved snouts and small mouths (Kullander, 1988), although Ploeg (1991) considered *Teleocichla* as part of the *C. wallacii* species group

Table 3 Pairwise Schoener's (above diagonal) and Pianka's (below diagonal) niche overlap indices within the Uruguay River species flock based on gut content analysis.

	celidochilus	*missioneira*	*minuano*	*tendybaguassu*	*hadrostigma*
celidochilus		0.80	0.09	0.09	0.09
missioneira	0.97		0.12	0.12	0.14
minuano	0.03	0.06		0.34	0.31
tendybaguassu	0.10	0.16	0.42		0.75
hadrostigma	0.09	0.16	0.38	0.95	

also based on morphology, focusing on their shared diminutive body sizes. We recovered the *C. wallacii* species group as the sister group to the clade containing the *C. lugubris* and *C. saxatilis* species groups, and the *Teleocichla* clade as the sister group to the clade containing those three species groups (Fig. 1) as in Piálek *et al.* (2012). These relationships were consistent between concatenated (ML and BI) and species tree analyses and across matrices of various degrees of missing data (Figs S3, S4 and S5). Members of the *C. wallacii* species group often inhabit leaf litter within small creeks (Montaña & Winemiller, 2009), whereas *Teleocichla* inhabit rocky rapids of large rivers (Kullander, 1988; Varella *et al.*, 2016). Therefore, these two groups likely evolved small body sizes in parallel; however, their positions in the phylogeny also suggest that small body sizes may have evolved once followed by the evolution of large-bodied species.

The rapid rise of species flocks

The rise of species flocks in lakes is a hallmark of cichlid evolution, including extensive radiations throughout East Africa (Wagner *et al.*, 2012, 2013; Seehausen, 2015) as well as small radiations in Africa and Middle America (Schliewen *et al.*, 2001; Elmer *et al.*, 2014; Ford *et al.*, 2016); however, such modes of evolution are conspicuously absent from rivers, which tend to be immigration-assembled rather than speciation-assembled (Seehausen, 2015). Species flocks did arise in the lower Congo River (Schwarzer *et al.*, 2011, 2012; Stiassny & Alter, 2015), with the species likely diversifying in allopatry via isolation among rapids and other hydrological and topographical barriers. However, these clades do not exhibit dramatic patterns of morphological and ecological diversification associated with lake-dwelling adaptive radiations (Schwarzer *et al.*, 2011, 2012; Seehausen, 2015; Stiassny & Alter, 2015; Alter *et al.*, 2017).

In previous analyses, based largely on mitochondrial loci, the relationships among species as well as the monophyly of species within the URSF were unresolved (Kullander *et al.*, 2010; Piálek *et al.*, 2012), and this poor resolution was largely attributed to their shallow divergence times (~1.2 My; Piálek *et al.*, 2012). Using hundreds of UCE loci, we show that most species are monophyletic with high support; however, the relationships among species remain elusive (Fig. 2). For example, *C. missioneira* and *C. minuano* were the only species not recovered as monophyletic by the Splitstree network (Fig. 2d), and the clustered co-ancestry analysis based on SNPs extracted from UCE loci revealed a higher genetic affinity between them, as indicated by the relatively large shared co-ancestry between individuals from these two species. Other species (i.e. *C. tendybaguassu* and *C. celidochilus*), on the other hand, showed long and well-supported branches in the Splitstree network analysis coupled with large amounts of shared co-ancestry among all their individuals. These variable levels of intrapopulation co-ancestry are likely a reflection of differences in evolutionary and demographic histories, such as different degrees of isolation, local selection regimes or effective population sizes (Malinsky *et al.*, 2016; Egger *et al.*, 2017).

In combination with species-specific head and pharyngeal jaw morphologies and associated trophic roles, our molecular results are consistent with ecologically based speciation among incipient species. In particular, the lack of accumulation of significant genetic differentiation among species, and considerable recent shared ancestry between some individuals, suggests that there is likely gene flow within the URSF. Furthermore, the reticulation observed in the phylogenetic network between *C. missioneira* and *C. minuano* could be due to events such as hybridization or recombination, among others (Huson & Bryant, 2006). Hybridization often occurs after colonization events and may predispose populations to adaptive radiation by increasing their responses to disruptive and divergent selection (Seehausen, 2004). In these situations, hybridization likely generates (or maintains) sufficient genomic variation, including at functional loci and, by extension, ecologically relevant traits that would permit populations to explore available adaptive peaks. For example, hybrids are often ecologically different than either parent species (Parsons *et al.*, 2011) and therefore have different potential to utilize opportunities afforded by the environment that can ultimately lead to the colonization of different adaptive peaks (Seehausen, 2004; Genner & Turner, 2012). Therefore, hybridization has not only played an important role in the adaptive radiations in Lakes Malawi (Joyce *et al.*, 2011; Malinsky *et al.*, 2017) and Tanganyika (Salzburger *et al.*, 2002; Koblmüller *et al.*, 2010; Meyer *et al.*, 2015, 2017), but also it has

been hypothesized that it may serve as major substrate from which adaptive radiations arise (Seehausen, 2005).

Rapid ecological diversification

After the colonization of lakes, cichlids have repeatedly diversified into species-rich assemblages that exhibit dramatic morphological and ecological diversity, and in many cases, similar suites of ecomorphs have arisen in each lake (Wagner *et al.*, 2012; Seehausen, 2015). We show that a small radiation of five riverine species of *Crenicichla* have rapidly diversified into five discrete ecomorphs associated with different trophic roles (Fig. 3). This diversity arose rapidly, such that these species are more ecologically differentiated than they are genetically differentiated, likely representing incipient ecological speciation. Furthermore, this clade has diversified along familiar environmental gradients.

Adaptive radiations among lake-dwelling cichlids have used a few ecological axes extensively and repeatedly during their proliferation, namely the benthic-to-pelagic habitat axis and the soft-bodied-to-hard-shelled prey axis (Kidd *et al.*, 2006; Cooper *et al.*, 2010; Muschick *et al.*, 2012; Hulsey *et al.*, 2013; Kusche *et al.*, 2014; Seehausen & Wagner, 2014). The URSF has utilized both of these axes during their radiation. Although most species are associated with benthic habitat and benthic-oriented prey items such as insects, molluscs and periphyton, *C. celidochilus* specializes upon small schooling fishes that occupy open waters (i.e. Characidae; Burress *et al.*, 2013a). Likewise, although most species consume either soft-bodied prey items or fishes, *C. minuano* specializes upon molluscs, including both bivalves and snails (Burress *et al.*, 2013a). *Crenicichla missioneira* is intermediate along both axes. For example, they consume a mixture of benthic- and pelagic-oriented fishes as well as moderately hard-bodied macrocrustaceans (Burress *et al.*, 2013a). Although *C. minuano* and *C. missioneira* are each other's closest relatives (Fig. 2), they have dramatically different head and LPJ morphologies associated with their highly divergent diets (Fig. 3).

The URSF exhibits highly specialized trophic adaptations that permit the exploitation of resources that would otherwise be inaccessible. For example, molluscs impose functional demands such as the necessity to generate sufficient biting force and the ability to withstand the associated structural stress incurred during the shell crushing process (Hulsey *et al.*, 2008). These adaptations usually involve reinforcement of the pharyngeal jaw bones and the development of molariform teeth (Burress, 2016). *Crenicichla minuano* has one of the most robust LPJs among cichlids (Burress, 2015), characterized by short processes and relatively few, robust, molariform teeth (Fig. 3f), which are specialized for crushing the shells of bivalves and snails (Fig. 3e). On the opposite end of the spectrum, piscivores often exhibit atrophied LPJs with long processes (Burress *et al.*, 2015), which is likely in response to gape limitations imposed by pharyngeal jaws that can constrain feeding efficiency in piscivores (McGee *et al.*, 2015). This morphology is exhibited by *Crenicichla celidochilus*, which is a specialist piscivore (Fig. 3). Lastly, hypertrophied lips, such as those exhibited by *C. tendybaguassu*, are a rare phenotype among cichlids; however, they have conspicuously evolved in all major clades of cichlids, including in Lakes Tanganyika, Malawi and Victoria (reviewed in Burress, 2015). Hypertrophied lips are also a polymorphism frequently associated with incipient species pairs (Elmer *et al.*, 2010; Colombo *et al.*, 2013; Manousaki *et al.*, 2013; Machado-Schiaffino *et al.*, 2014). Their trophic function is associated with foraging from rocky crevices (Baumgarten *et al.*, 2015). Indeed, *C. tendybaguassu* consumes primarily rock-associated insects (Burress *et al.*, 2013a; Fig. 3e).

Rapid transitions to herbivory are rare among fishes (Seehausen & Wagner, 2014), likely due to the physiological constraints associated with digesting nutrient-poor resources (Burress *et al.*, 2016 and references therein); however, in Lakes Tanganyika and Malawi, cichlids have extensively diversified into primary producer-associated trophic roles such as algae grazers (Danley & Kocher, 2001; Wagner *et al.*, 2009; Muschick *et al.*, 2012), which, among other trophic roles, has led to convergence in trophic-associated morphologies in these two lakes (Kocher *et al.*, 1993). The evolution of algae grazing is often associated with small, compact jaws (Winemiller *et al.*, 1995) and sometimes jaws that are conspicuously benthic-oriented (Ford *et al.*, 2016). Herbivory has also rapidly evolved within the URSF and in association with predictable changes in head, jaw and mouth morphology. *Crenicichla hadrostigma* grazes algae, probably directly from rock surfaces because their guts lacked detritus and sediment that might indicate a nongrazing mode of feeding (Fig. 3e) that characterizes many other geophagines (i.e. substrate sifting; Burress, 2015, 2016). Algae grazing has likely evolved in concert with their compact, benthic-oriented jaws (Fig. 3a,f) as in lake-dwelling clades in which herbivory has rapidly evolved (Ford *et al.*, 2016).

Species flocks replicated in lakes and rivers

We demonstrate that lake-like adaptive radiations have occurred among pike cichlids in the Uruguay River, where five species have evolved rapidly in syntopy in response to trophic-associated mechanisms. Seehausen (2015) discussed several factors that might explain the paucity of such adaptive radiations in rivers, including physical differences between lakes and rivers that might influence the ecological opportunities and therefore evolutionary results in each ecosystem. The obvious spatial disparity between rivers and lakes is the depth

dimension offered by lakes, which is hypothesized to play a major role during diversification of lake-dwelling cichlids (Seehausen & Magalhaes, 2010) and fishes in general (Seehausen & Wagner, 2014). Secondly, rocky shorelines and reefs associated with many of the East African Great Lakes may provide sufficient conditions for primary producer-associated trophic roles (e.g. algae grazers). Lastly, heterogeneous and unstable conditions associated with rivers are hypothesized to favour the evolution of omnivory (Jepsen & Winemiller, 2002 and references therein), and thus, there may not be suitable conditions for *in situ* ecological speciation and the subsequent evolution of specialization (Nosil, 2012). It is unclear how the URSF overcame these barriers, but several possibilities exist: (1) the paucity of other cichlid (and noncichlid) lineages in subtropical South American streams may have provided a competitive release (Albert *et al.*, 2011), (2) their colonization of a unique adaptive optimum among Neotropical cichlids associated with elongate tubular bodies (López-Fernández *et al.*, 2013) may have opened new evolutionary opportunities, (3) the shallow nature of the Uruguay River that may have permitted the evolution of primary producer-associated trophic roles and (4) gene flow that may maintain a diverse genetic substrate for selection (Seehausen, 2005) may have allowed this clade to overcome ecological and evolutionary constraints and thereby facilitated their attainment of novel adaptive opportunities. Whatever the case, the URSF lineage is an excellent example of a rapid and diverse cichlid radiation in a river system that in many ways parallels other cichlid radiations that are typically restricted to lacustrine environments.

Data archiving

Raw read data are archived in the NCBI Sequence Repository Archive (SRA; BioProject ID PRJNA396208), and concatenated and individual gene alignments are archived on Dryad (doi:10.5061/dryad.7qs13). Accession numbers for voucher specimens used in the molecular and morphological aspects of this study are available in the Supporting Information.

Acknowledgments

We are grateful to Mark Sabaj and Luiz Malabarba for kindly sharing tissues and Wilson S. Serra and Daniel Hernandez for assistance with fieldwork in Uruguay. Mark Sabaj kindly contributed the photograph of *T. monogramma*. Feedback from two anonymous reviewers and an Editor improved this paper. Fishes were collected in Uruguay in accordance with La Dirección Nacional de Recursos Acuáticos (DINARA) Permit #13/2014. This research was supported by the Jim Smith Endowment Fund from the Ohio Cichlid Association (to E.D.B) and National Science Foundation DEB #1354149 (to P.C.). This is Contribution No. 867 of the Auburn University Museum of Natural History.

References

Albert, J.S., Bart, H.L. Jr & Reis, R.E. 2011. Species richness and cladal diversity. In: *Historical Biogeography of Neotropical Freshwater Fishes* (J.S. Albert & R.E. Reis, eds), pp. 89–104. University of California Press, Berkeley, California.

Alter, S.E., Munshi-South, J. & Stiassny, M.L.J. 2017. Genomewide SNP data reveal cryptic phylogeographic structure and microallopatric divergence in a rapids-adapted clade of cichlids from the Congo River. *Mol. Ecol.* **26**: 1401–1419.

Arbour, J.H. & López-Fernández, H. 2014. Adaptive landscape and functional diversity of Neotropical cichlids: implications for the ecology and evolution of Cichlinae (Cichlidae; Cichliformes). *J. Evol. Biol.* **27**: 2431–2442.

Barluenga, M., Stölting, K.N., Salzburger, W., Muschick, M. & Meyer, A. 2006. Sympatric speciation in Nicaraguan crater lake cichlid fish. *Nature* **439**: 719.

Baumgarten, L., Machado-Schiaffino, G., Henning, F. & Meyer, A. 2015. What big lips are good for: on the adaptive function of repeatedly evolved hypertrophied lips of cichlid fishes. *Biol. J. Linn. Soc.* **115**: 448–455.

Bejerano, G., Pheasant, M., Makunin, I., Stephen, S., Kent, W.J., Mattick, J.S. *et al.* 2004. Ultraconserved elements in the human genome. *Science* **304**: 1321–1325.

Bolger, A.M., Lohse, M. & Usadel, B. 2014. Trimmomatic: a flexible trimmer for Illumina sequence data. *Bioinformatics* **30**: 2114–2120.

Burress, E.D. 2012. *Food web structure of a subtropical South American stream with particular focus on the co-evolution of form and function in an endemic species flock* (M.S. Thesis, Appalachian State University).

Burress, E.D. 2015. Cichlid fishes as models of ecological diversification: patterns, mechanisms, and consequences. *Hydrobiologia* **748**: 7–27.

Burress, E.D. 2016. Ecological diversification associated with the pharyngeal jaw diversity of Neotropical cichlid fishes. *J. Anim. Ecol.* **85**: 302–313.

Burress, E.D., Duarte, A., Serra, W.S., Loueiro, M., Gangloff, M.M. & Siefferman, L. 2013a. Functional diversification within a predatory species flock. *PLoS One* **8**: e80929.

Burress, E.D., Duarte, A., Serra, W.S., Gangloff, M.M. & Siefferman, L. 2013b. Species-specific ontogenetic diet shifts among Neotropical *Crenicichla*: using stable isotopes and tissue stoichiometry. *J. Fish Biol.* **82**: 1904–1915.

Burress, E.D., Duarte, A., Serra, W.S. & Loureiro, M. 2015. Rates of piscivory predict pharyngeal jaw morphology in a piscivorous lineage of cichlid fishes. *Ecol. Freshw. Fish* **25**: 590–598.

Burress, E.D., Holcomb, J.M. & Armbruster, J.W. 2016. Ecological clustering within a diverse minnow assemblage according to morphological, dietary and isotopic data. *Freshw. Biol.* **61**: 328–339.

Chakrabarty, P. 2004. Cichlid biogeography: comment and review. *Fish Fish.* **5**: 97–119.

Chifman, J. & Kubatko, L. 2014. Quartet inference from SNP data under the coalescent model. *Bioinformatics* **30**: 3317–3324.

Chifman, J. & Kubatko, L. 2015. Identifiability of the unrooted species tree topology under the coalescent model with time-reversible substitution processes, site-specific rate variation, and invariable sites. *J. Theor. Biol.* **374**: 35–47.

Colombo, M., Diepeveen, E.T., Muschick, M., Santos, M.E., Indermaur, A., Boileau, N. *et al.* 2013. The ecological and genetic basis of convergent thick-lipped phenotypes in cichlid fishes. *Mol. Ecol.* **22**: 670–684.

Cooper, W.J., Parsons, K., McIntyre, A., Kern, B., McGee-Moore, A. & Albertson, R.C. 2010. Bentho-pelagic divergence of cichlid feeding architecture was prodigious and consistent during multiple adaptive radiations within African rift-lakes. *PLoS One* **5**: e9551.

Crawford, N.G. & Faircloth, B.C. 2014. Cloudforest: code to calculate species trees from large genomic datasets. https://doi.org/10.5281/zenodo.12259.

Danley, P.D. & Kocher, T.D. 2001. Speciation in rapidly diverging systems: lessons from Lake Malawi. *Mol. Ecol.* **10**: 1075–1086.

Egger, B., Rösti, M., Böhne, A., Roth, O. & Salzburger, W. 2017. Demography and genome divergence of lake and stream populations of an East African cichlid fish. *Mol. Ecol.* **26**: 5016–5030.

Elmer, K.R., Lehtonen, T.K., Kautt, A.F., Harrod, C. & Meyer, A. 2010. Rapid sympatric ecological differentiation of crater lake cichlid fishes within historic times. *BMC Biol.* **8**: 1.

Elmer, K.R., Fan, S., Kusche, H., Spreitzer, M.L., Kautt, A.F., Franchini, P. *et al.* 2014. Parallel evolution of Nicaraguan crater lake cichlid fishes via non-parallel routes. *Nat. Comm.* **5**: 5168.

Faircloth, B.C. 2016. PHYLUCE is a software package for the analysis of conserved genomic loci. *Bioinformatics* **32**: 786–788.

Faircloth, B.C. & Glenn, T.C. 2012. Not all sequence tags are created equal: designing and validating sequence identification tags robust to indels. *PLoS One* **7**: e42543.

Faircloth, B.C., McCormack, J.E., Crawford, N.G., Harvey, M.G., Brumfield, R.T. & Glenn, T.C. 2012. Ultraconserved elements anchor thousands of genetic markers spanning multiple evolutionary timescales. *Syst. Biol.* **61**: 717–726.

Faircloth, B.C., Sorenson, L., Santini, F. & Alfaro, M.E. 2013. A phylogenomic perspective on the radiation of ray-finned fishes based upon targeted sequencing of ultraconserved elements (UCEs). *PLoS One* **8**: e65923.

Feilich, K.L. 2016. Correlated evolution of body and fin morphology in the cichlid fishes. *Evolution* **70**: 2247–2267.

Ford, A.G., Rüber, L., Newton, J., Dasmahapatra, K.K., Balarin, J.D., Bruun, K. *et al.* 2016. Niche divergence facilitated by fine-scale ecological partitioning in a recent cichlid fish adaptive radiation. *Evolution* **70**: 2718–2735.

Friedman, M., Keck, B.P., Dornburg, A., Eytan, R.I., Martin, C.H., Hulsey, C.D. *et al.* 2013. Molecular and fossil evidence place the origin of cichlid fishes long after Gondwanan rifting. *Proc. R. Soc. B* **280**: 20131733.

Genner, M.J. & Turner, G.F. 2012. Ancient hybridization and phenotypic novelty within Lake Malawi's cichlid fish radiation. *Mol. Biol. Evol.* **29**: 195–206.

Genner, M.J., Seehausen, O., Lunt, D.H., Joyce, D.A., Shaw, P.W., Carvalho, G.R. *et al.* 2007. Age of cichlids: new dates for ancient lake fish radiations. *Mol. Biol. Evol.* **24**: 1269–1282.

Gotelli, N.J. 2000. Null model analysis of species co-occurrence patterns. *Ecology* **81**: 2606–2621.

Grabherr, M.G., Haas, B.J., Yassour, M., Levin, J.Z., Thompson, D.A., Amit, I. *et al.* 2011. Full-length transcriptome assembly from RNA-Seq data without a reference genome. *Nat. Biotechnol.* **29**: 644–652.

Grossman, G.D. 1986. Food resources partitioning in a rocky intertidal fish assemblage. *J. Zool.* **1**: 317–355.

Grossman, G.D., Moyle, P.B. & Whitaker, J.O. Jr 1982. Stochasticity in structural and functional characteristics of an Indiana stream fish assemblage: a test of community theory. *Am. Nat.* **120**: 423–454.

Huelsenbeck, J.P. & Ronquist, F. 2001. MrBayes: Bayesian inference of phylogeny. *Bioinformatics* **17**: 754–755.

Hulsey, C.D., Roberts, R.J., Lin, A.S., Guldberg, R. & Streelman, J.T. 2008. Convergence in a mechanically complex phenotype: detecting structural adaptations for crushing in cichlid fish. *Evolution* **62**: 1587–1599.

Hulsey, C.D., Roberts, R.J., Loh, Y.H., Rupp, M.F. & Streelman, J.T. 2013. Lake Malawi cichlid evolution along a benthic/limnetic axis. *Ecol. Evol.* **3**: 2262–2272.

Huson, D.H. & Bryant, D. 2006. Application of phylogenetic networks in evolutionary studies. *Mol. Biol. Evol.* **23**: 254–267.

Jepsen, D.B. & Winemiller, K.O. 2002. Structure of tropical river food webs revealed by stable isotope ratios. *Oikos* **96**: 46–55.

Joyce, D.A., Lunt, D.H., Genner, M.J., Turner, G.F., Bills, R. & Seehausen, O. 2011. Repeated colonization and hybridization in Lake Malawi cichlids. *Curr. Biol.* **21**: R108–R109.

Katoh, K. & Standley, D.M. 2013. MAFFT multiple sequence alignment software version 7: improvements in performance and usability. *Mol. Biol. Evol.* **30**: 772–780.

Kidd, M.R., Kidd, C.E. & Kocher, T.D. 2006. Axes of differentiation in the bower-building cichlids of Lake Malawi. *Mol. Ecol.* **15**: 459–478.

Koblmüller, S., Egger, B., Sturmbauer, C. & Sefc, K.M. 2010. Rapid radiation, ancient incomplete lineage sorting and ancient hybridization in the endemic Lake Tanganyika cichlid tribe Tropheini. *Mol. Phylogenet. Evol.* **55**: 318–334.

Kocher, T.D., Conroy, J.A., McKaye, K.R. & Stauffer, J.R. 1993. Similar morphologies of cichlid fish in Lakes Tanganyika and Malawi are due to convergence. *Mol. Phylogenet. Evol.* **2**: 158–165.

Kullander, S.O. 1988. *Teleocichla*, a new genus of South American rheophilic cichlid fishes with six new species (Teleostei: Cichlidae). *Copeia* **1988**: 196–230.

Kullander, S.O. & Lucena, C.A.S. 2006. A review of the species of *Crenicichla* (Teleostei: Cichlidae) from the Atlantic coastal rivers of southeastern Brazil from Bahia to Rio Grande do Sul States, with descriptions of three new species. *Neotrop. Ichthyol.* **4**: 127–146.

Kullander, S.O., Norén, M., Friðriksson, G.B. & Lucena, C.A.S. 2010. Phylogenetic relationships of species of *Crenicichla* (Teleostei: Cichlidae) from southern South America based on the mitochondrial cytochrome b gene. *J. Zool. Syst. Evol. Res.* **48**: 248–258.

Kusche, H., Recknagel, H., Elmer, K.R. & Meyer, A. 2014. Crater lake cichlids individually specialize along the benthic–limnetic axis. *Ecol. Evol.* **4**: 1127–1139.

Lawson, D.J., Hellenthal, G., Myers, S. & Falush, D. 2012. Inference of population structure using dense haplotype data. *PLoS Genet.* **8**: e1002453.

Li, H. & Durbin, R. 2009. Fast and accurate short read alignment with Burrows-Wheeler transform. *Bioinformatics* **25**: 1754–1760.

Li, H., Handsaker, B., Wysoker, A., Fennell, T., Ruan, J., Homer, N. *et al.* 2009. The sequence alignment/map format and SAMtools. *Bioinformatics* **25**: 2078–2079.

López-Fernández, H., Winemiller, K.O. & Honeycutt, R.L. 2010. Multilocus phylogeny and rapid radiations in Neotropical cichlid fishes (Perciformes: Cichlidae: Cichlinae). *Mol. Phylogenet. Evol.* **55**: 1070–1086.

López-Fernández, H., Arbour, J.H., Winemiller, K.O. & Honeycutt, R.L. 2013. Testing for ancient adaptive radiations in neotropical cichlid fishes. *Evolution* **67**: 1321–1337.

de Lucena, C.A.S. 2007. Two new species of the genus *Crenicichla* Heckel, 1840 from the upper rio Uruguay drainage (Perciformes: Cichlidae). *Neotrop. Ichthyol.* **5**: 449–456.

de Lucena, C.A.S. & Kullander, S.O. 1992. The *Crenicichla* (Teleostei: Cichlidae) species of the Uruguai River drainage in Brazil. *Ichthyol. Explor. Fresh.* **3**: 97–192.

Machado-Schiaffino, G., Henning, F. & Meyer, A. 2014. Species-specific differences in adaptive phenotypic plasticity in an ecologically relevant trophic trait: hypertrophic lips in Midas cichlid fishes. *Evolution* **68**: 2086–2091.

Maddison, W.P. 1991. Squared-change parsimony reconstructions of ancestral states for continuous-valued characters on a phylogenetic tree. *Syst. Biol.* **40**: 304–314.

Maddison, W.P. & Maddison, D.R. 2011. Mesquite: a modular system for evolutionary analysis. 2011; Version 2.75.

Malinsky, M., Trucchi, E., Lawson, D. & Falush, D. 2016. RADpainter and fineRADstructure: population inference from RADseq data. *BioRxiv* 057711. https://doi.org/10.1101/057711.

Malinsky, M., Svardal, H., Tyers, A.M., Miska, E.A., Genner, M.J., Turner, G.F. *et al.* 2017. Whole genome sequences of Malawi cichlids reveal multiple radiations interconnected by gene flow. *BioRxiv* 143859. https://doi.org/10.1101/143859

Manousaki, T., Hull, P.M., Kusche, H., Machado-Schiaffino, G., Franchini, P. & Harrod, C. 2013. Parsing parallel evolution: ecological divergence and differential gene expression in the adaptive radiations of thick-lipped Midas cichlid fishes from Nicaragua. *Mol. Ecol.* **22**: 650–669.

Marcais, G. & Kingsford, C. 2011. A fast, lock-free approach for efficient parallel counting of occurrences of k-mers. *Bioinformatics* **27**: 764–770.

Martin, C.H., Cutler, J.S., Friel, J.P., Dening Touokong, C., Coop, G. & Wainwright, P.C. 2015. Complex histories of repeated gene flow in Cameroon crater lake cichlids cast doubt on one of the clearest examples of sympatric speciation. *Evolution* **69**: 1406–1422.

Matschiner, M., Musilová, Z., Barth, J.M., Starostová, Z., Salzburger, W., Steel, M. *et al.* 2017. Bayesian phylogenetic estimation of clade ages supports trans-Atlantic dispersal of cichlid fishes. *Syst. Biol.* **66**: 3–22.

McGee, M.D., Borstein, S.R., Neches, R.Y., Buescher, H.H., Seehausen, O. & Wainwright, P.C. 2015. A pharyngeal jaw evolutionary innovation facilitated extinction in Lake Victoria cichlids. *Science* **350**: 1077–1079.

McKenna, A., Hanna, M., Banks, E., Sivachenko, A., Cibulskis, K., Kernytsky, A. *et al.* 2010. The genome analysis toolkit: a MapReduce framework for analyzing next-generation DNA sequencing data. *Genome Res.* **20**: 1297–1303.

McMahan, C.D., Chakrabarty, P., Sparks, J.S., Smith, W.L. & Davis, M.P. 2013. Temporal patterns of diversification across global cichlid biodiversity (Acanthomorpha: Cichlidae). *PLoS One* **8**: e71162.

Meier, J.I., Marques, D.A., Mwaiko, S., Wagner, C.E., Excoffier, L. & Seehausen, O. 2017. Ancient hybridization fuels rapid cichlid fish adaptive radiations. *Nat. Commun.* **8**: 14363.

Meyer, B.S., Matschiner, M. & Salzburger, W. 2015. A tribal level phylogeny of Lake Tanganyika cichlid fishes based on a genomic multi-marker approach. *Mol. Phylogenet. Evol.* **83**: 56–71.

Meyer, B.S., Matschiner, M. & Salzburger, W. 2017. Disentangling incomplete lineage sorting and introgression to refine species-tree estimates for Lake Tanganyika cichlid fishes. *Syst. Biol.* **66**: 531–550.

Montaña, C.G. & Winemiller, K.O. 2009. Comparative feeding ecology and habitats use of *Crenicichla* species (Perciformes: Cichlidae) in a Venezuelan floodplain river. *Neotrop. Ichthyol.* **7**: 267–274.

Muschick, M., Indermaur, A. & Salzburger, W. 2012. Convergent evolution within an adaptive radiation of cichlid fishes. *Curr. Biol.* **22**: 2362–2368.

Newman, C.E. & Austin, C.C. 2016. Sequence capture and next-generation sequencing of ultraconserved elements in a large-genome salamander. *Mol. Ecol.* **25**: 6162–6174.

Nosil, P. 2012. *Ecological Speciation*. Oxford University Press, Oxford.

Parsons, K.J., Son, Y.H. & Albertson, R.C. 2011. Hybridization promotes evolvability in African cichlids: connections between transgressive segregation and phenotypic integration. *Evol. Biol.* **38**: 306–315.

Piálek, L., Říčan, O., Casciotta, J., Almirón, A. & Zrzavý, J. 2012. Multilocus phylogeny of *Crenicichla* (Teleostei: Cichlidae), with biogeography of the *C. lacustris* group: species flocks as a model for sympatric speciation in rivers. *Mol. Phylogenet. Evol.* **62**: 46–61.

Piálek, P., Dragova, K., Casciotta, J., Almirón, A. & Říčan, O. 2015. Description of two new species of *Crenicichla* (Teleostei: Cichlidae) from the lower Iguazu River with a taxonomic reappraisal of *C. iguassuensis*, *C. tesay*, and *C. yaha*. *Historia Nat.* **5**: 5–27.

Pianka, E.R. 1973. The structure of lizard communities. *Annu. Rev. Ecol. Evol. Syst.* **4**: 53–74.

Ploeg, A. 1991. *Revision of the South American Cichlid Genus Crenicichla* Heckel, 1840 with Descriptions of Fifteen new Species and Considerations on Species Groups, Phylogeny and Biogeography (Pisces, Perciformes, Cichlidae). Universiteit van Amsterdam, Academisch Proefschrift.

Rambaut, A., Suchard, M.A., Xie, D. & Drummond, A.J. 2014. Tracer v.1.6- MCMC Trace Analysis Tool. http://beast.bio.ed.ac.uk/Tracer.

Reclus, E. 1893. *The Earth and Its Inhabitants: South America*, Vol. **2**, Amazonia and La Plata. Appleton and Company, New York, NY, USA.

Revell, L.J., Johnson, M.A., Schulte, J.A., Kolbe, J.J. & Losos, J.B. 2007. A phylogenetic test for adaptive convergence in rock-dwelling lizards. *Evolution* **61**: 2898–2912.

Rohland, N. & Reich, R. 2012. Cost-effective, high-throughput DNA sequencing libraries for multiplexed target capture. *Genome Res.* **22**: 939–946.

Rohlf, F.J. 2004. tpsUtil, version 1.44. State University of New York, Stony Brook.

Rohlf, F.J. 2006. tpsDig2, version 2.1. State University of New York, Stony Brook.

Rohlf, F.J. 2007. tpsRelw, version 1.45. Department of Ecology and Evolution, State University of New York, Stony Brook.

Ronquist, F. & Huelsenbeck, J.P. 2003. MRBAYES 3: Bayesian phylogenetic under mixed models. *Bioinformatics* **19**: 1572–1574.

Salzburger, W., Baric, S. & Sturmbauer, C. 2002. Speciation via introgressive hybridization in East African cichlids? *Mol. Ecol.* **11**: 619–625.

Schliewen, U., Rassmann, K., Markmann, M., Markert, J., Kocher, T. & Tautz, D. 2001. Genetic and ecological divergence of a monophyletic cichlid species pair under fully sympatric conditions in Lake Ejagham, Cameroon. *Mol. Ecol.* **10**: 1471–1488.

Schluter, D. 2000. *The Ecology of Adaptive Radiation*. Oxford University Press, Oxford.

Schoener, T.W. 1970. Nonsynchronous spatial overlap of lizards in patchy habitats. *Ecology* **51**: 408–418.

Schwarzer, J., Misof, B., Ifuta, S.N. & Schliewen, U.K. 2011. Time and origin of cichlid colonization of the lower Congo rapids. *PLoS One* **6**: e22380.

Schwarzer, J., Misof, B. & Schliewen, U.K. 2012. Speciation within genomic networks: a case study based on *Steatocranus* cichlids of the lower Congo rapids. *J. Evol. Biol.* **25**: 138–148.

Seehausen, O. 2004. Hybridization and adaptive radiation. *Trends Ecol. Evol.* **19**: 198–207.

Seehausen, O. 2015. Process and pattern in cichlid radiations–inferences for understanding unusually high rates of evolutionary diversification. *New Phytol.* **207**: 304–312.

Seehausen, O. & Magalhaes, I.S. 2010. Geographical mode and evolutionary mechanism of ecological speciation in cichlid fish. In: *In Search of the Causes of Evolution* (P. Grant & R. Grant, eds), pp. 282–308. Princeton University Press, Princeton, NJ, USA.

Seehausen, O. & Wagner, C.E. 2014. Speciation in freshwater fishes. *Annu. Rev. Ecol. Evol. Syst.* **45**: 621–651.

Serra, W.S., Duarte, A., Burress, E.D. & Loureiro, M. 2011. Perciformes, Cichlidae, *Crenicichla tendybaguassu* Lucena and Kullander, 1992: first record for Uruguay. *Check List* **7**: 357–359.

Shafer, A. & Wolf, J.B. 2013. Widespread evidence for incipient ecological speciation: a meta-analysis of isolation-by-ecology. *Ecol. Lett.* **16**: 940–950.

Sidlauskas, B. 2008. Continuous and arrested morphological diversification in sister clades of characiform fishes: a phylomorphospace approach. *Evolution* **62**: 3135–3156.

Simpson, G.G. 1953. *The Major Features of Evolution*. Columbia University Press, New York.

Smith, B.T., Harvey, M.G., Faircloth, B.C., Glenn, T.C. & Brumfield, R.T. 2014. Target capture and massively parallel sequencing of ultraconserved elements for comparative studies at shallow evolutionary time scales. *Syst. Biol.* **63**: 83–95.

Snir, S. & Rao, S. 2012. Quartet MaxCut: a fast algorithm for amalgamating quartet trees. *Mol. Phylogenet. Evol.* **62**: 1–8.

Sparks, J.S. & Smith, W.L. 2005. Freshwater fishes, dispersal ability, and nonevidence: "Gondwana life rafts" to the rescue. *Syst. Biol.* **54**: 158–165.

Stamatakis, A. 2006. RAxML-VI-HPC: maximum likelihood-based phylogenetic analyses with thousands of taxa and mixed models. *Bioinformatics* **22**: 2688–2690.

Stiassny, M.L. & Alter, S.E. 2015. Phylogenetics of *Teleogramma*, a riverine clade of African cichlid fishes, with a description of the deepwater molluskivore-*Teleogramma obamaorum*-from the lower reaches of the Middle Congo River. *Am. Mus. Novit.* **3831**: 1–18.

Swofford, D.L. 2003. PAUP*. Phylogenetic analysis using parsimony (* and Other Methods). Version 4. Sinauer Associates, Sunderland, Massachusetts.

Varella, H.R., Zuanon, J., Kullander, S.O. & López-Fernández, H. 2016. *Teleocichla preta*, a new species of cichlid from the Rio Xingu Basin in Brazil (Teleostei: Cichlidae). *J. Fish Biol.* **89**: 1551–1569.

Wagner, C.E., McIntyre, P.B., Buels, K.S., Gilbert, D.M. & Michel, E. 2009. Diet predicts intestine length in Lake Tanganyika's cichlid fishes. *Funct. Ecol.* **23**: 1122–1131.

Wagner, C.E., Harmon, L.J. & Seehausen, O. 2012. Ecological opportunity and sexual selection together predict adaptive radiation. *Nature* **487**: 366–369.

Wagner, C.E., Keller, I., Wittwer, S., Selz, O.M., Mwaiko, S., Greuter, L. *et al.* 2013. Genome-wide RAD sequence data provide unprecedented resolution of species boundaries and relationships in the Lake Victoria cichlid adaptive radiation. *Mol. Ecol.* **22**: 787–798.

Wainwright, P.C., Smith, W.L., Price, S.A., Tang, K.L., Sparks, J.S., Ferry, L.A. *et al.* 2012. The evolution of pharyngognathy: a phylogenetic and functional appraisal of the pharyngeal jaw key innovation in labroid fishes and beyond. *Syst. Biol.* **61**: 1001–1027.

Winemiller, K.O. 1989. Ontogenetic diet shifts and resource partitioning among piscivorous fishes in the Venezuelan llanos. *Environ. Biol. Fish.* **26**: 177–199.

Winemiller, K.O., Kelso-Winemiller, L.C. & Brenkert, A.L. 1995. Ecomorphological diversification and convergence in fluvial cichlid fishes. *Environ. Biol. Fish.* **44**: 235–261.

Yoder, J.B., Clancey, E., Des Roches, S., Eastman, J.M., Gentry, L., Godsoe, W. *et al.* 2010. Ecological opportunity and the origin of adaptive radiations. *J. Evol. Biol.* **23**: 1581–1596.

Zhang, J. 2004. *Quantitative Ecology*. Science Press, Beijing.

Supporting information

Additional Supporting Information may be found online in the supporting information tab for this article:

Figure S1 Hypotheses of the relationships among *Crenicichla* species groups based on morphology.

Figure S2 Landmark schemes used to quantify (left) body and (right) lower pharyngeal jaw shape: homologous (red) and sliding (purple) landmarks.

Figure S3 Concatenated Maximum likelihood *Crenicichla* phylogenies based on data sets with different proportions of missing data (a-d). Nodal support was assessed by 500 non-parametric bootstrap replicates.

Figure S4 Bayesian inference *Crenicichla* phylogenies based on data sets with different proportions of missing data (a–d). Nodal support was assessed by 500 non-parametric bootstrap replicates.

Figure S5 Species trees (SVDquartets) *Crenicichla* phylogenies based on data sets with different proportions of missing data (a–d). Nodal support was assessed by 500 non-parametric bootstrap replicates.

Table S1 Voucher specimens used for molecular analyses.

Table S2 Voucher specimens used for geometric morphometric analyses.

Data deposited at Dryad: https://doi.org/10.5061/dryad.7qs13.

Received 17 May 2017; revised 13 August 2017; accepted 12 October 2017